


Cite this: *RSC Adv.*, 2023, 13, 9595

# Hexafluoroisopropanol-based deep eutectic solvents for high-performance DNA extraction†

Jia Xu,  Yuan Yang, Xiaonan Cai and Han Xiao \*

In this study, hexafluoroisopropanol (HFIP)-based deep eutectic solvents (DESs) were developed and used for DNA extraction from human whole blood samples for the first time. HFIP-based DESs were prepared using HFIP and choline chloride (ChCl)/tetrabutylammonium chloride/cetyltrimethylammonium bromide as the hydrogen bond donor and acceptor, respectively. The two-phase system formation was promoted with different inorganic salts as the phase-forming component. According to the strong phase separation capability and high DNA extraction efficiency, DESs consisting of HFIP/ChCl-(NH<sub>4</sub>)<sub>2</sub>SO<sub>4</sub>, HFIP/ChCl-Na<sub>2</sub>SO<sub>4</sub> and HFIP/ChCl-MgSO<sub>4</sub> were then selected for application in DNA extraction. The factors that could have impacted the DNA extraction process, including molar ratio of DES, DES addition, salt species and addition, and sample pH, were systematically investigated *via* single-factor experimental analysis. Furthermore, we selectively examined bovine serum albumin and RNA to assess the specificity of the HFIP-based DESs for DNA extraction. Conclusively, 93.9%, 96.7% and 99.8% DNA could be extracted using the HFIP/ChCl-(NH<sub>4</sub>)<sub>2</sub>SO<sub>4</sub>, HFIP/ChCl-Na<sub>2</sub>SO<sub>4</sub>, and HFIP/ChCl-MgSO<sub>4</sub> systems, respectively. Moreover, the developed systems were successfully used to extract DNA from human whole blood with satisfactory results. The DNA secondary structure was stable after DES extraction with the electrostatic interaction between DES and DNA as the main force driving DNA adsorption by DES.

Received 16th January 2023  
Accepted 19th March 2023

DOI: 10.1039/d3ra00315a

rsc.li/rsc-advances

## Introduction

Nucleic acid purification and enrichment are crucial for conducting reliable research in genetic profiling, clinical trials, and food safety.<sup>1–3</sup> Nucleic acid extraction is a complex process, as proteins and polysaccharides in cells and the environment disturb the purification of nucleic acids, and high concentrations of enzymes can also degrade nucleic acids.<sup>4</sup> Conventional DNA purification methods (such as phenol-chloroform liquid–liquid extraction) require the extensive use of organic solvents, which are not environmentally friendly.<sup>5</sup> Commercialized DNA extraction kits require repeated elution and centrifugation steps, which may result in the loss of DNA. Therefore, it is of great significance to develop new DNA purification and separation technologies that are economical, efficient, environmentally-friendly, and easy to operate.

Aqueous two-phase systems (ATPSs) are mild, biocompatible, and environmentally-friendly liquid–liquid extraction, separation, and purification techniques that have been extensively used in biotechnological applications.<sup>6,7</sup> Polymer/polymer, polymer/salt, and small molecular alcohol/salt constituents are commonly used in the development of

ATPSs.<sup>8–10</sup> These functions on the principle of spontaneous phase separation, which occurs between two distinct water-soluble compounds above a certain concentration. A high content of both phase components in water can provide a biocompatible environment for bioactive components, thus protecting their structural integrity and biological activity.<sup>11–13</sup> The demand for environmentally friendly solvents led to the use of deep eutectic solvents (DESs) in extraction processes. Generally, DESs are typically prepared with two components, hydrogen bond donors (HBDs) and hydrogen bond acceptors (HBAs), with the aid of heating and stirring.<sup>14,15</sup> The formed eutectic mixtures generally exhibit much lower melting points than those of their individual components. Compared with traditional organic solvents, DESs have low toxicity, and high thermal stability, are non-volatile, and can readily dissolve many organic and inorganic compounds.<sup>16</sup> They have abundant functional groups, that can attract target compounds by hydrogen bonding and hydrophobic interactions.<sup>17–20</sup> DESs have recently been used in analytical chemistry as effective extractants for the separation and preconcentration of analytes from a variety of complex matrices, such as biological fluid, food and environmental samples.<sup>21–23</sup> DESs are excellent solvents for DNA.<sup>24</sup> Mondal *et al.* studied the solubility and stability of DNA in bio-based DESs and found that DNA is soluble as well as chemically and structurally stable in DESs.<sup>24</sup>

Hexafluoroisopropanol (HFIP), a strong HBD (1.96), much larger than that of water (1.02), can aid in the preparation of

*Institute of Maternal and Child Health, Wuhan Children's Hospital (Wuhan Maternal and Child Healthcare Hospital), Tongji Medical College, Huazhong University of Science & Technology, Wuhan, 430016, China. E-mail: tjxiaohan@hust.edu.cn*

† Electronic supplementary information (ESI) available. See DOI: <https://doi.org/10.1039/d3ra00315a>



DESs with a variety of HBAs.<sup>25–27</sup> HFIP-based DESs have been successfully employed in the purification of pesticides, anthraquinones, and dyes<sup>25–27</sup> and are also used as environmental reaction media.<sup>28</sup> In this study, we synthesized HFIP-based DESs and used them for the extraction and quantification of DNA for the first time. Three types of HFIP-based DESs were directly synthesized and applied in the rapid and efficient extraction of DNA from spiked aqueous solution and human whole blood samples. To comprehensively understand the ability of DESs to extract DNA, the proportions of DESs components were explored in detail, including those of HBD species and inorganic salts. HFIP/ChCl DESs and three types of sulfates were then used to investigate the influencing factors and back-extraction performance. Bovine serum albumin (BSA) and RNA were used to assess the specificity of the HFIP-based DESs for DNA extraction. In addition, the HFIP/ChCl DES method was used to extract DNA from human whole blood samples to evaluate its practical applicability.

## Materials and methods

### Materials and reagents

HFIP was purchased from Aladdin Chemistry Co., Ltd. (Shanghai, China). Choline chloride (ChCl), tetrabutylammonium chloride (TBAC), cetyltrimethylammonium bromide (CTAB), salmon sperm DNA sodium salt, ribonucleic acid (yeast) (RNA) and BSA were purchased from Macklin (Shanghai, China).  $(\text{NH}_4)_2\text{SO}_4$ ,  $\text{K}_2\text{HPO}_4$ ,  $\text{KH}_2\text{PO}_4$ ,  $\text{Na}_2\text{CO}_3$ ,  $\text{Na}_2\text{HPO}_4$ ,  $\text{Na}_2\text{SO}_4$ ,  $\text{MgSO}_4$ , hydrochloric acid (HCl), ammonia solution (25–28%, w/v) and ethylenediaminetetraacetic acid disodium salt dehydrate ( $\text{EDTA}\cdot\text{Na}_2\cdot 2\text{H}_2\text{O}$ ) were purchased from Sino-pharm Chemical Reagent, Co., Ltd. (Shanghai, China). Tris-hydrochloride (Tris-HCl) was purchased from Guangzhou Saigu Biotech Co., Ltd (Guangzhou, China). All other chemicals used were of analytical reagent grade and were not further purified unless otherwise indicated. Deionized water (18.25 M $\Omega$ ) was used in all experiments.

Human whole blood samples from healthy volunteers were provided by the Wuhan Children's Hospital (China). Appropriate amounts of anticoagulant were added to the blood samples which were then stored at  $-20\text{ }^\circ\text{C}$  until use.

### Instruments

Agitation and extraction were accomplished using a UXI orbital shaker (Huxi, Shanghai, China). The DNA concentrations of the solution were determined using an ultraviolet-1600PC UV-Vis spectrophotometer (XIPU, Shanghai, China) with a 1.0 cm quartz cell. DNA amplification was performed using a T100™ thermal cycler (Bio-Rad Laboratories, USA). The polymerase chain reaction (PCR) products were analyzed using 1.5% agarose gel electrophoresis with ethidium bromide staining followed by visualization on ChemiDoc XRS+ Imaging System (Bio-Rad Laboratories, USA). Fourier-transform infrared (FT-IR) spectra were recorded using a 470FT-IR spectrometer (Thermo Nicolet, USA) at room temperature. The  $^1\text{H}$ - $^1\text{H}$  nuclear Overhauser spectroscopy (NOESY) and  $^1\text{H}$  nuclear magnetic

resonance ( $^1\text{H}$  NMR) spectra were obtained using an Avance NEO 400 MHz spectrometer (Bruker, Germany). Circular dichroism (CD) spectra were obtained using JASCO J-1500 (JASCO, Japan). Dynamic light scattering (DLS) was evaluated using a Zeta sizer Nano ZS90 (Malvern, England).

### DESs synthesis

Three kinds of DESs were synthesized based on ChCl, TBAC, and CTAB used as HBAs and HFIP as the HBD. HBA and HBD were placed in a screw-cap pressure tube at a designed molar ratio. The mixture was then heated at  $80\text{ }^\circ\text{C}$  for 2 h with constant magnetic stirring until a homogeneous and stable liquid formed. All the prepared DESs were stored at room temperature for usage.

### DNA partitioning

The phase-forming components were essential for DNA partitioning. Various two-phase systems consisting of 0.5 mL DES (HBA and HFIP molar ratio of 1 : 2) and 0.8 g inorganic salts were prepared in 5 mL of TE buffer (pH 7.0). The DNA concentration was  $10\text{ }\mu\text{g mL}^{-1}$ . The solution was then vigorously mixed using an orbital shaker and left to equilibrate for 10 min. After full phase separation, the phase behavior was recorded and the DNA concentration in the bottom phase was quantified using a UV-Vis spectrophotometer at 260 nm.

### DNA extraction

To evaluate the extraction performance of the proposed HFIP/ChCl DES, several influencing factors, including the HBA : HBD molar ratio, DES addition, salt addition, and solution pH, were explored.

An appropriate amount of inorganic salt was dissolved in 5 mL TE buffer with a certain amount of DNA ( $10\text{ }\mu\text{g mL}^{-1}$ ). A certain volume of DES was then added. The mixture was mixed well and left to stand for 10 min to allow it to separate into two phases. The bottom phase was withdrawn using a microsyringe and diluted with methanol at four times the phase volume. The DNA concentration in the bottom phases was determined at 260 nm using a UV-Vis spectrophotometer. Additionally, a blank sample without DNA was analyzed in the same system to eliminate any background effects.

The DNA extraction efficiency (%) and phase ratio were calculated according to the following formulas:

$$\text{extraction efficiency (\%)} = \left( \frac{C_f \times V_f}{C_0 \times V_0} \right) \times 100\%$$

$$\text{phase ratio} = \left( \frac{V_f}{V_0} \right)$$

where,  $C_0$  is the spiked DNA concentration and  $C_f$  is the DNA concentration in the DES-rich phase after extraction.  $V_0$  is the volume of the DNA sample and  $V_f$  is the volume of the DES-rich phase.



## Sample preparation

A human whole blood sample (200  $\mu\text{L}$ ) was mixed with proteinase K (20  $\mu\text{L}$ , 100  $\text{mg mL}^{-1}$ ) and Triton X-100 (20  $\mu\text{L}$ ) and the mixture was incubated at 70  $^{\circ}\text{C}$  for 10 min. The mixture was then diluted to 1 mL in TE buffer (pH 8.0). After centrifugation at 12 000 rpm for 2 min, the supernatant (900  $\mu\text{L}$ ) was mixed with the same volume of anhydrous methanol. After another 2 min centrifugation cycle, the supernatant (1 mL) was mixed with 4 mL of TE buffer (pH 8.0). Then,  $(\text{NH}_4)_2\text{SO}_4$  (1.4 g),  $\text{Na}_2\text{SO}_4$  (0.6 g), or  $\text{MgSO}_4$  (1.2 g) was added to the solution and the mixture was stirred well. Finally, DES (0.7 mL) was added to the mixture. The system was allowed to stand for 10 min to allow the DNA to be completely partitioned between the two phases. Finally, 200  $\mu\text{L}$  of the bottom phase was withdrawn using a microsyringe and transferred to a 1.5 mL vial with 400  $\mu\text{L}$  of distilled water. The mixture was vortexed and incubated at 90  $^{\circ}\text{C}$  for 5 min and then centrifuged to achieve complete separation. The clear and transparent supernatant was directly used as the DNA template for PCR.

## Results and discussion

The FT-IR spectra and  $^1\text{H}$  NMR results were used to confirm the formation of hydrogen bonds in the synthesized HFIP-based DESs. The FT-IR characterization of all the prepared HFIP-based DESs is shown in Fig. 1. The stretching vibration peaks of O–H in pure HFIP and ChCl were at 3424.98  $\text{cm}^{-1}$  and 3293.82  $\text{cm}^{-1}$ , respectively, which shifted to a lower wavenumber of 3165.54  $\text{cm}^{-1}$  at in ChCl/HFIP. This was due to the reduction in the force constant caused by the transfer of the electron cloud of the oxygen atom to the hydrogen bond. The shift in the –OH stretching vibration indicated the existence of hydrogen bonding between ChCl and HFIP. In addition, compared with the spectra of ChCl and HFIP, both characteristic peaks were distinguishable in the ChCl/HFIP spectra. Furthermore, no new peaks were detected, indicating that there was no chemical reaction during DES synthesis. A similar phenomenon was observed for FT-IR spectra of the other HFIP-based DESs, which confirmed the presence of hydrogen bonds in these DESs (Fig. 1b).

The NOESY spectrum was shown in Fig. S1.† The results showed there was a strong hydrogen bonding between O–H in HFIP and O–H in ChCl. The  $^1\text{H}$  NMR results of all of the prepared HFIP-based DESs are shown in Fig. S2.† The  $^1\text{H}$  NMR of CTAB-HFIP was as follows:  $\delta$  4.62 (s, 1H), 3.47 (m, 2H), 3.38 (s, 9H), 1.76 (s, 2H), 1.37 (s, 26H), and 0.9 (t, 3H). The  $^1\text{H}$  NMR of ChCl-HFIP was as follows:  $\delta$  4.60 (s, 1H), 4.01 (dd, 2H), 3.52 (m, 2H), and 3.21 (d, 9H). The  $^1\text{H}$  NMR of TBAC-HFIP was as follows:  $\delta$  4.53 (s, 1H), 3.11 (m, 8H), 1.36 (m, 8H), 1.32 (m, 8H), and 0.94 (t, 12H). The characteristic peaks are consistent with those reported previously.<sup>27,29</sup>

### DES selection

To evaluate the partitioning performance and ability of the established HFIP-based DESs (HFIP/ChCl, HFIP/TBAC, and HFIP/CTAB) to form phases, salmon sperm DNA was selected as a model molecule and seven types of inorganic salts ( $(\text{NH}_4)_2\text{SO}_4$ ,  $\text{K}_2\text{HPO}_4$ ,  $\text{KH}_2\text{PO}_4$ ,  $\text{Na}_2\text{CO}_3$ ,  $\text{Na}_2\text{HPO}_4$ ,  $\text{MgSO}_4$ , and  $\text{Na}_2\text{SO}_4$ ) were used as phase separation inducers. After phase separation to equilibrium, DNA was transferred to the bottom DES-rich phase, while the top phase contained mostly inorganic salts.

The DNA partitioning results are summarized in Table S1.† The HFIP/CTAB- $\text{Na}_2\text{CO}_3$  and HFIP/CTAB- $\text{K}_2\text{HPO}_4$  systems formed a homogeneous phase and could not achieve phase separation. The HFIP/CTAB- $\text{Na}_2\text{HPO}_4$  system was divided into three phases; thus, it could not achieve two-phase separation. The other solutions, including all of the HFIP/ChCl and HFIP/TBAC systems, HFIP/CTAB- $\text{Na}_2\text{SO}_4$ , HFIP/CTAB- $\text{KH}_2\text{PO}_4$ , HFIP/CTAB- $\text{MgSO}_4$ , and HFIP/CTAB- $(\text{NH}_4)_2\text{SO}_4$  achieved transparent liquid–liquid two-phase formation. In these two-phase systems, 50  $\mu\text{L}$  of the bottom phase was extracted with 200  $\mu\text{L}$  of water to support the extraction of DNA into the aqueous phase. After vortexing and centrifugation, the systems, including all of the HFIP/TBAC, HFIP/ChCl- $(\text{NH}_4)_2\text{SO}_4$ , HFIP/ChCl- $\text{MgSO}_4$ , HFIP/ChCl- $\text{K}_2\text{HPO}_4$ , HFIP/ChCl- $\text{Na}_2\text{CO}_3$ , HFIP/ChCl- $\text{Na}_2\text{HPO}_4$ , HFIP/ChCl- $\text{Na}_2\text{SO}_4$ , and HFIP/CTAB- $\text{MgSO}_4$  systems formed two phases with a clear boundary. The DNA concentration in the top aqueous phase was then measured using a UV-Vis spectrophotometer at 260 nm. It is showed that, in all of the HFIP/TBAC systems, and the HFIP/ChCl- $\text{K}_2\text{HPO}_4$ , HFIP/ChCl- $\text{Na}_2\text{CO}_3$ , HFIP/ChCl- $\text{Na}_2\text{HPO}_4$  and the HFIP/CTAB- $\text{MgSO}_4$  systems,

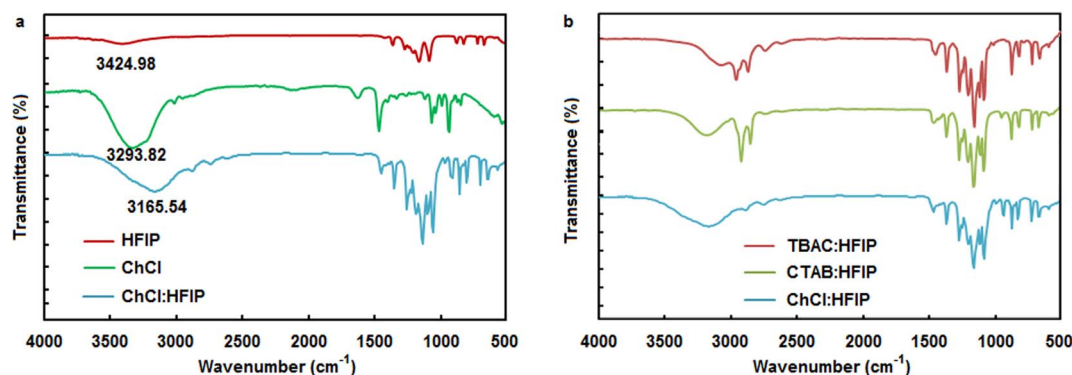


Fig. 1 The FT-IR spectra of HFIP, ChCl, ChCl/HFIP (a) and TBAC/HFIP, CTAB/HFIP, ChCl/HFIP (b).

almost no DNA can be detected in the bottom phase, indicating that there is no DNA transferring into the DES-rich phase. However, DNA recovered in the DES-rich phase was more than 50% in three systems including HFIP/ChCl-(NH<sub>4</sub>)<sub>2</sub>SO<sub>4</sub>, HFIP/ChCl-Na<sub>2</sub>SO<sub>4</sub>, and HFIP/ChCl-MgSO<sub>4</sub> systems, thus these systems were used in subsequent experiments.

### Effect of molar proportion of DES

Three types of DESs consisting of ChCl and HFIP with different molar ratios (1 : 1.5, 1 : 2, 1 : 3, and 1 : 4) were formed to explore their influence on DNA extraction. The distribution of DNA was mainly related to the relative affinity of the two phases. It can be seen from the phase ratio results (red lines) that the volume of bottom DES-rich phase increased as the proportion of HFIP in DES increased, leading to the change of DNA content in the DES-rich phase. For HFIP/ChCl-(NH<sub>4</sub>)<sub>2</sub>SO<sub>4</sub>, the extraction efficiency of DNA in the bottom phase increased as molar ratio varied from 1 : 1.5 to 1 : 3 and then decreased at the molar ratio of 1 : 4 (Fig. 2). The same phenomenon was observed in the HFIP/ChCl-Na<sub>2</sub>SO<sub>4</sub> and HFIP/ChCl-MgSO<sub>4</sub> systems. The optimal ChCl/HFIP molar ratio was selected at 1 : 3.

### Effect of inorganic salt concentration

The inorganic salts can be used as inducers for phase separation in two-phase systems, and can also affect the ionic strength and phase ratio. As shown in Fig. 3a, for HFIP/ChCl-(NH<sub>4</sub>)<sub>2</sub>SO<sub>4</sub>

system, the effects of the (NH<sub>4</sub>)<sub>2</sub>SO<sub>4</sub> addition in the range of 0.6–2.0 g was investigated. The system with 0.6 g (NH<sub>4</sub>)<sub>2</sub>SO<sub>4</sub> did not show separation into two phases. Regarding (NH<sub>4</sub>)<sub>2</sub>SO<sub>4</sub>, the DNA extraction efficiency increased as the concentration increased from 0.8 g to 1.4 g, while it exhibited a small decrease as the concentration exceeded 1.4 g. As for HFIP/ChCl-Na<sub>2</sub>SO<sub>4</sub> system, the Na<sub>2</sub>SO<sub>4</sub> concentration in the range of 0.4–1.6 g was investigated, 0.4 g Na<sub>2</sub>SO<sub>4</sub> could not induce the phase separation. The increasing addition of Na<sub>2</sub>SO<sub>4</sub> reduced the transfer of DNA into DES-rich phase; as a result, the extraction efficiency of DNA was decreased (Fig. 3b). Thus, 0.6 g of Na<sub>2</sub>SO<sub>4</sub> was sufficient for DNA extraction. In the HFIP/ChCl-MgSO<sub>4</sub> system, the MgSO<sub>4</sub> addition in the range of 0.4–2.0 g was investigated; 0.4 g MgSO<sub>4</sub> could not induce the phase separation. As shown in Fig. 3c, there was an increased change in the extraction of DNA when the concentration of MgSO<sub>4</sub> increased from 0.6 g to 1.2 g. Thereafter, a significant decrease was observed; thus, the optimum amount of MgSO<sub>4</sub> was 1.2 g.

### Effect of DES addition

The amount of DES is an essential parameter for DNA extraction. In the absence of DES, sufficient interactions could not occur between DES and DNA, but excess DES increased the solution viscosity to block DNA dispersion. The effects of DES addition on the DNA extraction efficiency are illustrated in Fig. 4. In the HFIP/ChCl-(NH<sub>4</sub>)<sub>2</sub>SO<sub>4</sub> and HFIP/ChCl-MgSO<sub>4</sub>

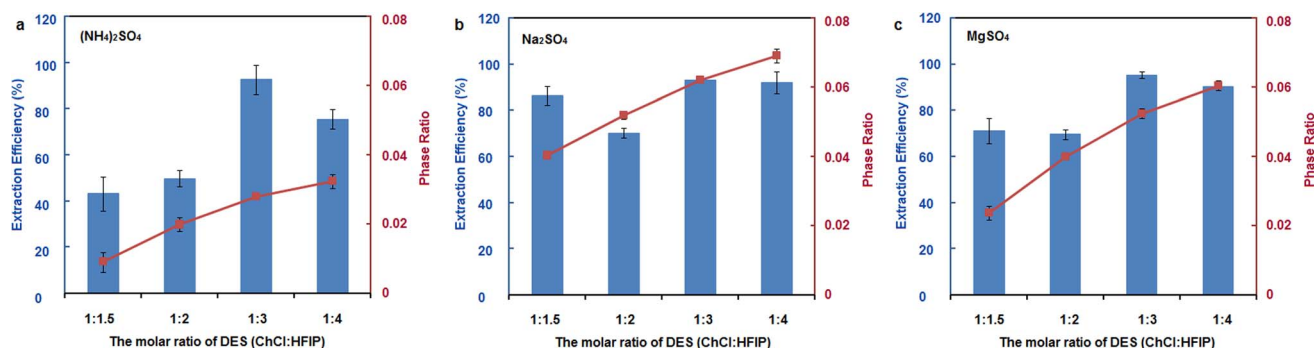


Fig. 2 The effects of molar ratio of DES (ChCl/HFIP) on extraction efficiency and phase ratio in HFIP/ChCl-(NH<sub>4</sub>)<sub>2</sub>SO<sub>4</sub> system (a), HFIP/ChCl-Na<sub>2</sub>SO<sub>4</sub> system (b), and HFIP/ChCl-MgSO<sub>4</sub> system (c).

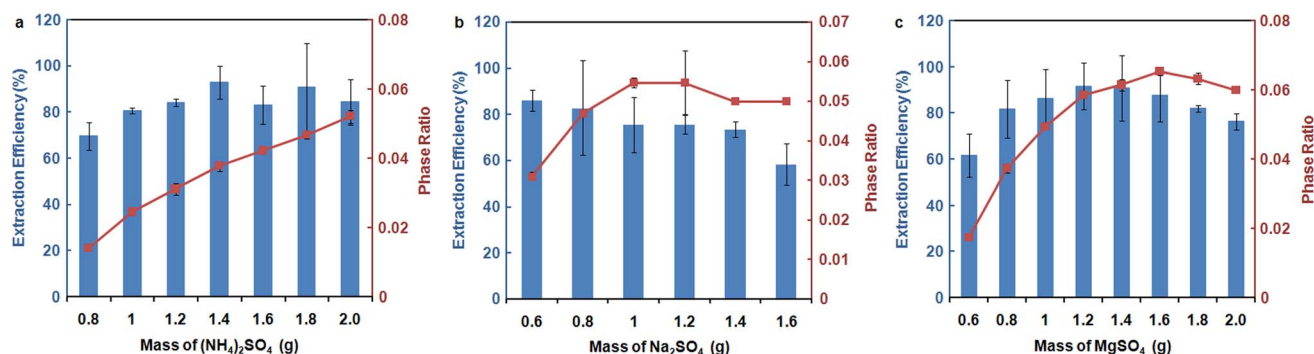


Fig. 3 The effects of (NH<sub>4</sub>)<sub>2</sub>SO<sub>4</sub> mass (a), Na<sub>2</sub>SO<sub>4</sub> mass (b), and MgSO<sub>4</sub> mass (c) on the extraction efficiency.





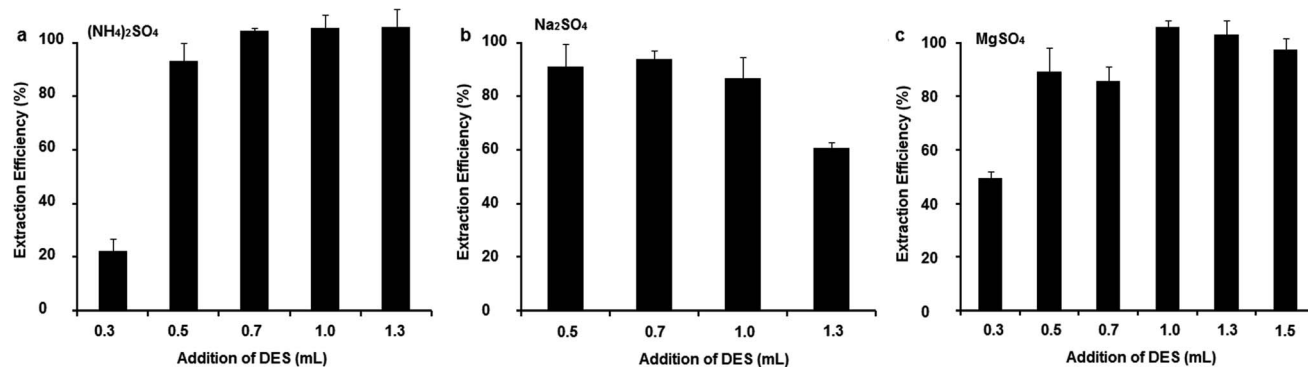


Fig. 4 The effects of DES addition on extraction efficiency in HFIP/ChCl- $(\text{NH}_4)_2\text{SO}_4$  system (a), HFIP/ChCl- $\text{Na}_2\text{SO}_4$  system (b), and HFIP/ChCl- $\text{MgSO}_4$  system (c).

systems, the DNA extraction efficiency increased with the amount of DES. However, as the amount of DES further increased, there was no significant increase in the extraction efficiency. Therefore, 0.7 mL and 1 mL DES were selected as the most suitable amount for the HFIP/ChCl- $(\text{NH}_4)_2\text{SO}_4$  and HFIP/ChCl- $\text{MgSO}_4$  systems. For HFIP/ChCl- $\text{Na}_2\text{SO}_4$  system, excess DES decreased the DNA extraction efficiency; 0.7 mL of DES was selected as appropriate amounts for subsequent experiments.

### Effect of sample pH

Considering that the solution pH can affect DES decomposition, and harsh pH conditions may compromise the structural integrity of DNA, the effect of pH on the extraction of DNA was investigated at pH values ranging from 2 to 9. TE buffer was used to adjust the solution pH. As shown in Fig. 5, the maximum peak areas were obtained at pH 8 for all of the studied systems; however, at other pH values, the extraction efficiency was lower. An alkaline medium was better for DNA extraction than an acidic medium in the HFIP/ChCl system, but the extraction efficiency decreased with a continuous increase in the pH. The extraction efficiency ranged from 73.8% to 93.9% for the HFIP/ChCl- $(\text{NH}_4)_2\text{SO}_4$  system, 71.5% to 96.7% in the HFIP/ChCl- $\text{Na}_2\text{SO}_4$  system, and 48.6% to 99.8% in HFIP/ChCl- $\text{MgSO}_4$  system as the sample pH ranged from 2 to 9, indicating

that the DNA was preferentially enriched in the DES-rich phase. The bottom phase had a higher affinity toward DNA, promoting its distribution in the DES-rich phase.

### Specificity

The purity of DNA directly determined the reliability and sensitivity of further downstream application. DNA, RNA, and protein contaminants must be separated. RNA (yeast) and BSA were selected as model interfering molecules, and  $10 \mu\text{g mL}^{-1}$  RNA or  $0.2 \text{ mg mL}^{-1}$  BSA was added to the three prepared HFIP/ChCl systems under the optimal conditions. We investigated the RNA and BSA extraction efficiencies under different pH conditions by adding RNA or BSA instead of DNA, to the systems. After the complete separation of the systems, the RNA or BSA in the DES-rich phase was diluted and analyzed. As shown in Fig. S3 and S4,† when the pH ranged from 2 to 9, the BSA extraction efficiency was lower than 49.9%, 47.7%, and 73.9% for HFIP/ChCl- $(\text{NH}_4)_2\text{SO}_4$ , HFIP/ChCl- $\text{Na}_2\text{SO}_4$ , and HFIP/ChCl- $\text{MgSO}_4$  systems, respectively. When the pH value ranged from 2 to 9, the RNA extraction efficiency was lower than 26.3%, 12.4%, and 19.6% for HFIP/ChCl- $(\text{NH}_4)_2\text{SO}_4$ , HFIP/ChCl- $\text{Na}_2\text{SO}_4$ , and HFIP/ChCl- $\text{MgSO}_4$  system, respectively. Under the optimum condition of pH 8.0, the BSA and RNA extraction efficiencies were below 43%, and 20%, respectively. RNA and

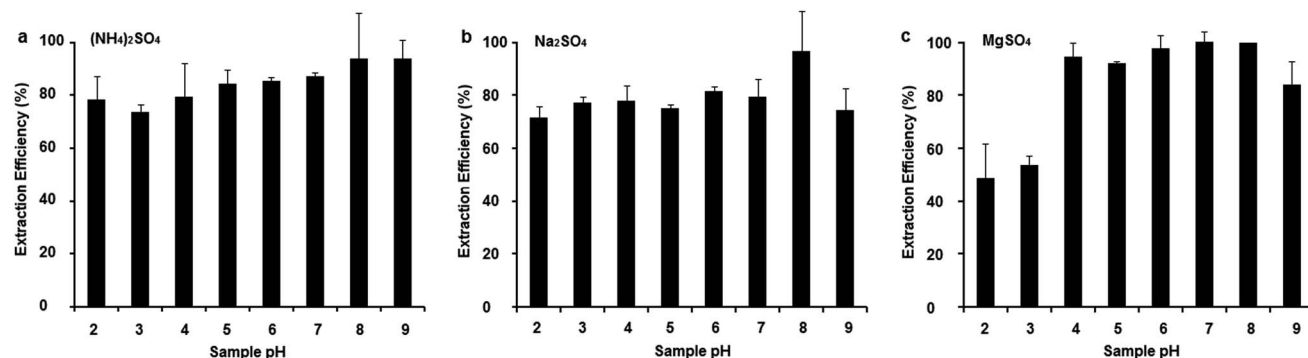


Fig. 5 The effects of solution pH on extraction efficiency in HFIP/ChCl- $(\text{NH}_4)_2\text{SO}_4$  system (a), HFIP/ChCl- $\text{Na}_2\text{SO}_4$  system (b), and HFIP/ChCl- $\text{MgSO}_4$  system (c).



BSA tended to transfer to the top aqueous phase in the studied HFIP/ChCl systems. The results showed that the HFIP/ChCl system had good selectivity for DNA.

### Analysis of human blood samples

After the first extraction process, 93.9%, 96.7% and 99.8% of the DNA in the HFIP/ChCl-(NH<sub>4</sub>)<sub>2</sub>SO<sub>4</sub>, HFIP/ChCl-Na<sub>2</sub>SO<sub>4</sub>, and HFIP/ChCl-MgSO<sub>4</sub> systems was extracted to the DES-rich phase under the optimum extraction conditions, respectively. The purification of DNA using DES-based extraction was intended to obtain high-purity DNA to meet the requirements of further downstream application. Therefore, the back-extraction process was carried out to back-extract the DNA to the aqueous phase. Herein, a human whole blood sample was selected for the separation process. After back-extraction, the recovered DNA in the aqueous phase was assayed by 1.5% agarose gel electrophoresis, as shown in Fig. S5.† The A260/A280 ratio of the

recovered DNA was in the range of 1.64 to 1.89. The DNA recovered *via* back extraction was directly used as a template for PCR. A 274 bp *TP53* gene fragment and a 335 bp *EGFR* gene fragment were amplified; the primer details are shown in Table S2.† The PCR mixtures (25 µL) consisted of 1 µL of recovered DNA, 0.5 µL each of the forward and reverse primers (10 mmol L<sup>-1</sup>), and 12.5 µL of Taq PCR Master Mix. The thermo cycling conditions were as follows: 10 min at 95 °C for denaturation, followed by 35 cycles of 95 °C for 30 s, 58 °C for 30 s, and 72 °C for 1 min. This was followed by a final holding step at 72 °C for 5 min. The analytical result is presented in Fig. S6.†

In addition, we compared the proposed HFIP-based DESs extraction method with a commercial DNA extraction kit (Tiangen Biotech, Beijing, China). For 200 µL of human whole blood, approximately 40 µg, 30 µg and 70 µg of DNA was recovered in the HFIP/ChCl-(NH<sub>4</sub>)<sub>2</sub>SO<sub>4</sub>, HFIP/ChCl-Na<sub>2</sub>SO<sub>4</sub> and HFIP/ChCl-MgSO<sub>4</sub> systems under the optimal conditions, respectively. However, approximately 3.5 µg of DNA was recovered by the commercial kit. The proposed method takes 30 min to extract DNA from human whole blood and involves four centrifugation steps and two standing steps. The method of commercial DNA extraction kit requires about 31 min for total extraction and consists of six centrifugation steps and three standing steps. The HFIP-based DESs extraction method proposed is simpler than the method of commercial kit, and requires similar extraction time. The results indicated that the proposed method could be applied to effectively extract DNA from human whole blood samples.

### Extraction mechanism

**CD spectra.** We next studied the secondary structure of DNA using CD analyses. The CD spectra of DNA before and after extraction (HFIP/ChCl-Na<sub>2</sub>SO<sub>4</sub> system) exhibited negative absorption at a wavelength 250 nm, corresponding to the characteristics of B-form DNA and positive absorption at 278 nm wavelength corresponding to  $\pi$ - $\pi$  base packing (Fig. 6).

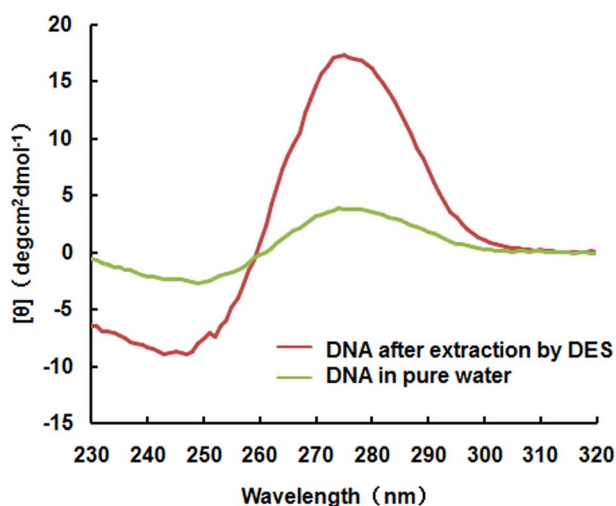


Fig. 6 CD spectra of DNA before and after extraction.

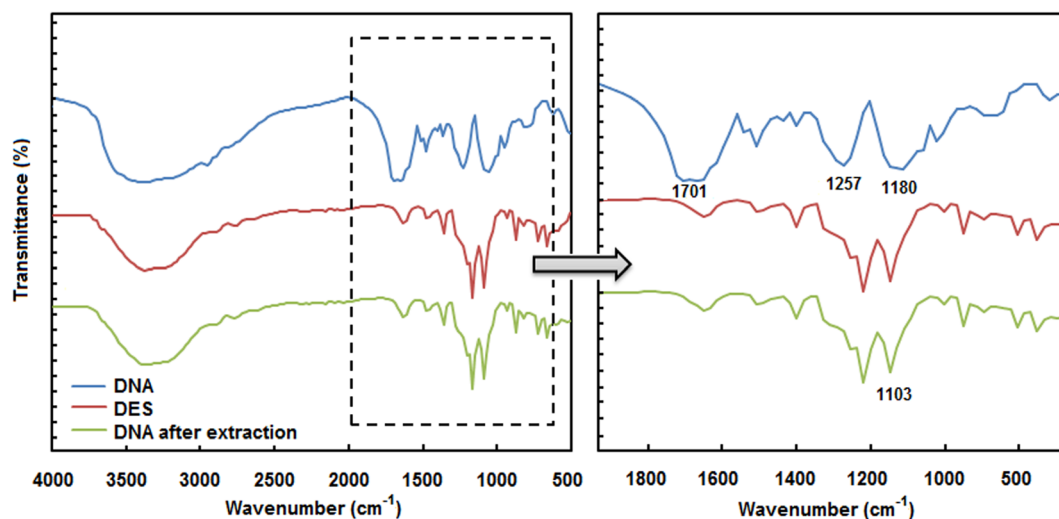


Fig. 7 The FT-IR spectra of HFIP/ChCl DES and DNA before and after extraction.



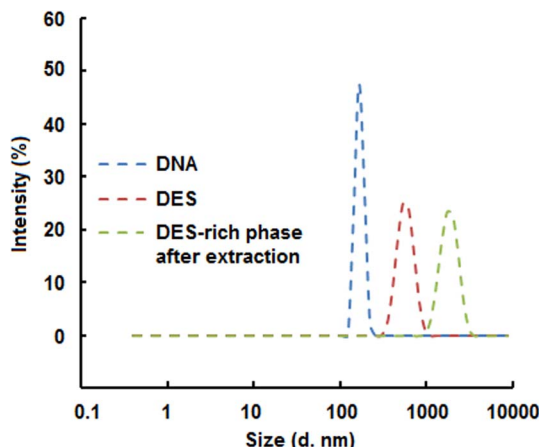


Fig. 8 Size-distribution of DNA, HFIP/ChCl DES, and DES-rich phase after extraction.

The conserved peaks showed that DNA did not undergo conformational changes after extraction.

**FT-IR spectra.** The extraction mechanism and binding characteristics between DNA and DES were investigated by recording the FT-IR spectra of DNA before and after extraction at room temperature. The characteristic FT-IR spectrum of DNA is shown in Fig. 7. The appearance of absorption bands at 1180 and 1257  $\text{cm}^{-1}$  was due to the symmetric and asymmetric stretching vibrations of the P-O bonds in the DNA phosphate groups. The absorption peak at 1701  $\text{cm}^{-1}$  was attributed to the stretching vibration of the C=O and C=N of the bases.<sup>24</sup> After the DNA was extracted to the DES-rich phase, the symmetric stretching vibration band attributed to the  $\text{PO}_2^{2-}$  groups at 1180  $\text{cm}^{-1}$  was not affected, whereas the asymmetric band at 1257  $\text{cm}^{-1}$  was found to have disappeared. These results indicated that an interaction occurred between ammonium chloride cations and the phosphate groups of DNA, which was caused by the electrostatic attraction between DNA and DES.

**DLS.** DLS, a common technique to determine particle size, was performed to scan the DNA solution (1  $\text{mg mL}^{-1}$ ), DES (HFIP/ChCl- $\text{Na}_2\text{SO}_4$  systems), and the DES-rich phase after extraction (diluted twice). The determinant hydrodynamic radius distributions were 164 nm, 531 nm, and 1718 nm for the DNA solution, DES solution, and DES-rich phase after extraction, respectively (Fig. 8). Hence, we suggest that larger aggregates were formed by DNA with DES after extraction. This may be due to the electrostatic interaction between DES and DNA.

## Conclusion

In this study, HFIP-based DESs were prepared with various HBAs, including ChCl, TBAC, and CTAB. The prepared HFIP/ChCl DES could help extract DNA quickly and efficiently. Under the optimized conditions, the maximum extraction efficiency for DNA was found to be more than 93% in the HFIP/ChCl DES systems. Moreover, it was also found that the HFIP/ChCl DES systems were beneficial enriching DNA, other than RNA and BSA. To some extent, the above DES systems achieved selective

DNA extraction. The proposed method was demonstrated with the extraction of DNA from a human whole blood sample. The DNA extracted using the HFIP/ChCl DES systems were suitable for PCR amplification. The extraction mechanism was also discussed. The results showed that the DNA secondary structure was stable after DES extraction and that the electrostatic interaction between DES and DNA was the main force driving DNA adsorption by DES. This approach provides a method for DNA extraction and a new direction for the development of DESs in the field of extraction and separation.

## Ethical statement

The authors state that all experiments were performed in compliance with the relevant laws and institutional guidelines. The human whole blood used in here was the remaining blood sample after routine clinical examination and the informed consent is exempted with the consent of the ethics committee of Wuhan Children's Hospital (Wuhan Maternal and Child Healthcare Hospital). This study has been approved by the ethics committee of this hospital (No. 2022R024-E03).

## Author contributions

Jia Xu: conceptualization, methodology, formal analysis, validation, writing-original draft. Yuan Yang: methodology, formal analysis, validation. Xiaonan Cai: methodology, formal analysis, validation. Han Xiao: project administration.

## Conflicts of interest

The authors declare no competing interests.

## Acknowledgements

This research was supported by the National Natural Science Foundation of China (Nos. 81802109).

## References

- 1 Y. Chen, Y. Liu, Y. Shi, J. Ping, J. Wu and H. Chen, *TrAC, Trends Anal. Chem.*, 2020, **127**, 115912.
- 2 M. N. Emaus, M. Varona, D. R. Eitzmann, S. Hsieh, V. R. Zeger and J. L. Anderson, *TrAC, Trends Anal. Chem.*, 2020, **130**, 115985.
- 3 A. G. Pérez, E. González-Martínez, C. R. D. Águila, D. A. González-Martínez, G. G. Ruiz, A. G. Artalejo and H. Yee-Madeira, *Colloids Surf., A*, 2020, **591**, 124500.
- 4 X. Wang, M. Liu, F. Peng and X. Ding, *J. Chromatogr. A*, 2021, **1659**, 462626.
- 5 T. Li, M. D. Joshi, D. R. Ronning and J. L. Anderson, *J. Chromatogr. A*, 2013, **1272**, 8–14.
- 6 K. K. Athira and R. L. Gardas, *Fluid Phase Equilib.*, 2022, **558**, 113463.
- 7 W. N. Phong, P. L. Show, Y. H. Chow and T. C. Ling, *J. Biosci. Bioeng.*, 2018, **126**(3), 273–281.

- 8 Y. Zhou, X. Yang, L. Bai, Z. Wu, J. Zhang, Z. Qin and J. Fan, *J. Mol. Liq.*, 2022, **368**, 120630.
- 9 X. H. Zhang, H. N. Cui, J. J. Zheng, X. D. Qing, K. L. Yang, Y. Q. Zhang, L. M. Ren, L. Y. Pan and X. L. Yin, *Food Res. Int.*, 2023, **163**, 112278.
- 10 Y. Chen, X. Liang and G. M. Kontogeorgis, *Sep. Purif. Technol.*, 2023, **306**, 122624.
- 11 K. Xu, Y. Wang, Y. Huang, N. Li and Q. Wen, *Anal. Chim. Acta*, 2015, **864**, 9–20.
- 12 P. Xu, Y. Wang, J. Chen, X. Wei, W. Xu, R. Ni, J. Meng and Y. Zhou, *Talanta*, 2018, **189**, 467–479.
- 13 F. Raji and A. Rahbar-Kelishami, *Colloids Surf., A*, 2021, **624**, 126823.
- 14 A. M. Ramezani, R. Ahmadi and Y. Yamini, *TrAC, Trends Anal. Chem.*, 2022, **149**, 116566.
- 15 P. Janicka, M. Kaykhani, J. Plotka-Wasyłka and J. Gębicki, *Green Chem.*, 2022, **24**, 5035.
- 16 Q. Zhang, K. O. Vigier, S. Royer and F. Jérôme, *Chem. Soc. Rev.*, 2012, **41**, 7108–7146.
- 17 M. M. Contreras-Gómez, Á. Galán-Martín, N. Seixas, A. M. C. Lopes, A. Silvestre and E. Castro, *Bioresour. Technol.*, 2023, **369**, 128396.
- 18 R. Rashid, S. M. Wani, S. Manzoor, F. A. Masoodi and M. M. Dar, *Food Chem.*, 2023, **398**, 133871.
- 19 O. Mokhodoeva, V. Maksimova, A. Shishov and V. Shkinev, *Sep. Purif. Technol.*, 2023, **305**, 122427.
- 20 F. Peng, M. Liu, X. Wang and X. Ding, *Anal. Chim. Acta*, 2021, **1181**, 338899.
- 21 F. Shakirova, A. Shishov and A. Bulatov, *Talanta*, 2021, **234**, 122660.
- 22 J. Cao, C. Wang, L. Shi, Y. Cheng, H. Hu, B. Zeng and F. Zhao, *Food Chem.*, 2022, **383**, 132586.
- 23 A. Duque, J. Grau, J. L. Benedé, R. M. Alonso, M. A. Campanero and A. Chisvert, *Talanta*, 2022, **243**, 123378.
- 24 D. Mondal, M. Sharma, C. Mukesh, V. Gupta and K. Prasad, *Chem. Commun.*, 2013, **49**, 9606–9608.
- 25 W. W. Deng, Y. Zong and Y. X. Xiao, *ACS Sustainable Chem. Eng.*, 2017, **5**, 4267–4275.
- 26 W. Deng, L. Yu, X. Li, J. Chen, X. Wang, Z. Deng and Y. Xiao, *Food Chem.*, 2019, **274**, 891–899.
- 27 K. Xu, P. Xu and Y. Wang, *Talanta*, 2020, **213**, 120839.
- 28 L. Wang, D. Dai, Q. Chen and M. He, *J. Fluorine Chem.*, 2014, **158**, 44–47.
- 29 M. Nemati, M. R. A. Mogaddam, M. A. Farazajdeh, M. Tuzen and J. Khandaghi, *J. Chromatogr. A*, 2021, **1660**, 462653.

